Chapter 2

The Manufacturing of Smart Foam and a Simple Source Radiation Control Application

2.1 Introduction

A smart foam noise suppression device, combining a distributed, piezoelectric active layer and a passive sound absorbing acoustic foam, is developed for the purpose of minimizing structural acoustic radiation. The primary motivating factor for the development of smart foam is to combine active and passive control strategies such that noise generated by vibrating structures can be efficiently attenuated over a broad range of frequencies. A schematic of the smart foam is shown in Figure 2.1 and shows a circular layer of sound absorbing foam with a physically curved PVDF actuator distributed through it's midsection. The piezoelectric actuator serves as the active control input possessing a control connection for electrical excitation. The curved configuration of the PVDF translates in-plane strain to out of plane motion, thereby, radiating sound away from the foam surface. The actuator performs as an acoustic control source, exciting the structural and acoustic phase of the foam, and performs best in the low-frequency region due to the necessary signal processing that is involved in active control. The secondary acoustic field generated by smart foam alters the acoustic radiation impedance of a

primary noise source creating a reduction in the total sound power. The most important advantage of implementing such a hybrid device in noise control applications is good, simultaneous low and high-frequency controller performance. Other positive attributes of active-passive noise control devices, in comparison to purely active control systems, are increased reliability, decreased control power and decreased control spillover. One can envision a host of noise control applications that could implement smart foam. The fact that it is a relatively lightweight and compact actuator indicates that it is a good candidate for aircraft noise control applications. For example, an array of smart foam modules may be adhered to the walls of an aircraft cabin to minimize noise due to turbulent atmospheric conditions or engine noise.

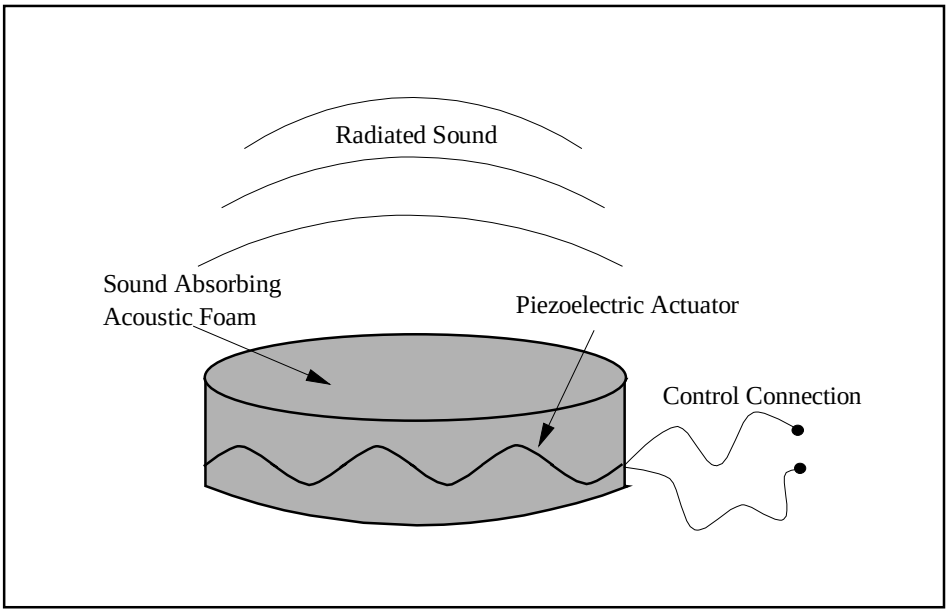

Figure 2.1: Illustration of smart foam active/passive noise control actuator.

The present chapter presents a description of the smart foam components and details the construction of the actuator for improved performance. The utility and performance of the active/passive device is demonstrated by controlling sound radiation from a vibrating, baffled piston. The problem of suppressing piston sound radiation is addressed because it represents a simple source and generates a monopole-like radiation pattern at low frequencies. A successful solution to this simple noise control problem

using smart foam has two advantages. It will provide insight into the fundamental method of operation of smart foam and represent an important step in the progression toward implementing smart foam in more complex noise control problems. One can interpret the vibration pattern of complex structures as a finite, independently phased array of monopole sources. Therefore, an array of smart foam elements can conceptually be employed to attenuate the sound generated by a complex structural noise source.

2.2 Smart Foam Components

It is important to note that the piezoelectric polymer film (PVDF) and polyurethane components of smart foam were chosen due to their acoustic impedance compatibility with air. Similar impedance characteristics are desirable between the components of an active/passive, distributed acoustic control device and the operating medium because it minimizes the amount of control energy needed. A host of other composite materials can be studied to develop alternative active/passive noise control strategies depending on the operating medium and the intended application. Recall that Howarth et al. [17] developed an underwater noise control device comprised of a passive, compliant elastomer matrix augmented with piezoceramic actuators and PVDF sensors. Their distributed, piezocomposite actuator was designed to minimize sound reflection from surfaces submerged in a heavy fluid, such as water, that are impinged upon by acoustic waves. The composite materials used for the actuator are appropriate due to the corrosion resistance of the elastomer in the heavy fluid medium and the similar impedance characteristics of the elastomer and piezoceramics when compared to water.

In this study, partially-reticulated polyurethane foam, provides the passive element of smart foam and it dissipates incident acoustic wave energy through friction associated with the relative motion of the liquid and solid phases of the foam. Partially-reticulated polyurethane foam is an acoustical grade, flexible ester-based urethane foam designed to give maximum sound absorption per given thickness [28]. The foam also acts as a host matrix that shields the piezoelectric actuator (which is driven by an electrical excitation) from the surrounding environment. The thickness of the acoustic foam used in this study

is 2.0 inches, which is a common, easily-handled thickness for most sound abatement materials.

Before discussing the details of the piezolectric component of smart foam, the "poling" process during the piezoelectric polymer manufacturing needs to be described. Furthermore, a brief summary of the fundamental behavior of piezoelectric films will be given.

To obtain significant piezoelectric activities, a piezoelectric film must be "poled". Poling exposes the film to a high electric field at elevated temperatures. The level of piezo activity obtained by poling depends upon poling time, field strength and temperature. When conducted properly, the poling process provides a permanent orientation of molecular dipoles within the polymer. Figure 2.2 depicts the poling direction in symbolic form with an arrow.

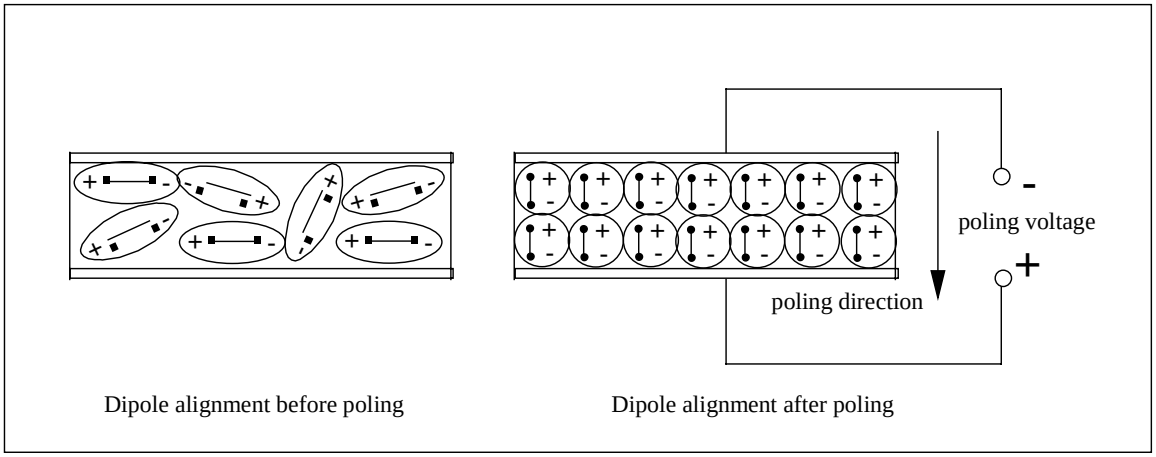

Figure 2.2: Piezo film dipole alignment.

When an external force applied to PVDF results in compressive or tensile strain, the film develops a proportionate open circuit voltage. Exposure to a reciprocating force results in a corresponding alternating electrical signal. This phenomena allows PVDF to be used in countless sensor applications such as machinery vibration monitoring and robotic tactile sensing. Conversely, a working voltage applied to the electrodes of PVDF causes the film to elongate or contract, depending on the polarity of the field. Exposed to an alternating field, the film elongates and contracts as the field polarity changes. This

mechanical action permits PVDF to be implemented in applications related to acoustic control actuation, as exhibited by smart foam, and active vibration dampening.

Piezoelectric materials are anisotropic and calculations involving piezo activity must account for this directionality. Conventions have been established for a systematic tabulation of properties. The films axis are identified by the numerals indicated in Figure 2.3 where: **1** corresponds to length, **2** to width, and **3** to thickness. Two subscripts are used. The first numeral always identifies the axis of applied electrical field. The second numeral refers to the axis of induced mechanical strain or applied stress. Use of this nomenclature will be seen in the following paragraph.

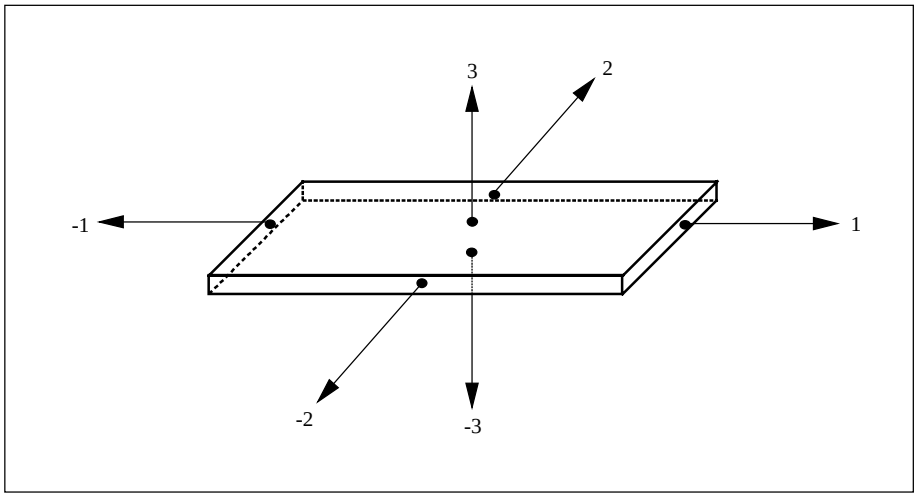

Figure 2.3: Numerical classification of piezo film axes.

The active input of smart foam is comprised of commercially manufactured PVDF and is available in sheets with various custom metallized surfaces and the thickness ranges from $9\,\mu m$ to $110\ \mu m$. The material can sustain a maximum applied voltage of 30 Volts ($V_{peak\ to\ peak}$) per μm. Silver-electroded PVDF film was chosen because it can sustain the high voltage amplitudes required for actuator applications without electrical breakdown. For the development of smart foam, a $28\,\mu m$ PVDF thickness is preferred because it limits the maximum input voltage to approximately 300 V_{rms}, which can be supplied by common laboratory amplifiers. Note that the term “rms” denotes the root mean square of the peak amplitude. Additionally, $28\,\mu m$ PVDF film is easily cut and

formed into different configurations. The piezoelectric strain constant d_{31}, which denotes the degree to which the piezoelectric material dimensions change relative to the applied field, has a value of $23x10^{-12}$ (m/m)/(V/m) [29].

2.3 Smart Foam Construction

The most prominent and unique feature of smart foam is the physically curved PVDF actuator that is embedded in the polyurethane foam matrix. The actuator, driven by an electrical control voltage, initiates motion of the structural and acoustic phases of the foam, and actively minimizes the sound created by a vibrating noise source. As stated previously, an oscillating voltage applied to the electrodes of piezoelectric film causes the film to elongate or contract as the field polarity changes. In a horizontal or flat configuration, this mechanical response occurs in-plane or along the length of the film. Note that the fundamental requirement for farfield sound propagation from a structural element is out-of-plane motion. Owing to this, a flat layer of PVDF film embedded within the foam would be ineffective as an acoustic control source. It is for these reasons that smart foam requires a curved design for the PVDF actuator which produces a vertical displacement component to the PVDF response under electrical excitation. This requirement manifests a countless number of possible designs for the actuator. For the following preliminary experimental studies, a PVDF actuator curved into a series of half-cylinders is chosen for the initial smart foam design. This configuration is perhaps the simplest curved shape to embed within the foam. Figure 2.4 indicates the motion of a single cylindrically-curved actuator of length L (represented by the bold curve) during mechanical expansion and contraction. Assuming an oscillating voltage is applied to the PVDF, curve 1 indicates the motion of the piezoelectric film during expansion and curve 2 denotes the motion of the piezoelectric film during contraction. Farfield sound radiation is attributed to the velocity of the surrounding air in the y direction. The velocity of the air is due to the differential displacement of the actuator defined by the shaded region bound by curve 1 and curve 2. The effects of the orientation of the PVDF actuator, relative to smart foam sound output, will be studied in more detail in Chapter 4 which deals with the numerical modeling of smart foam.

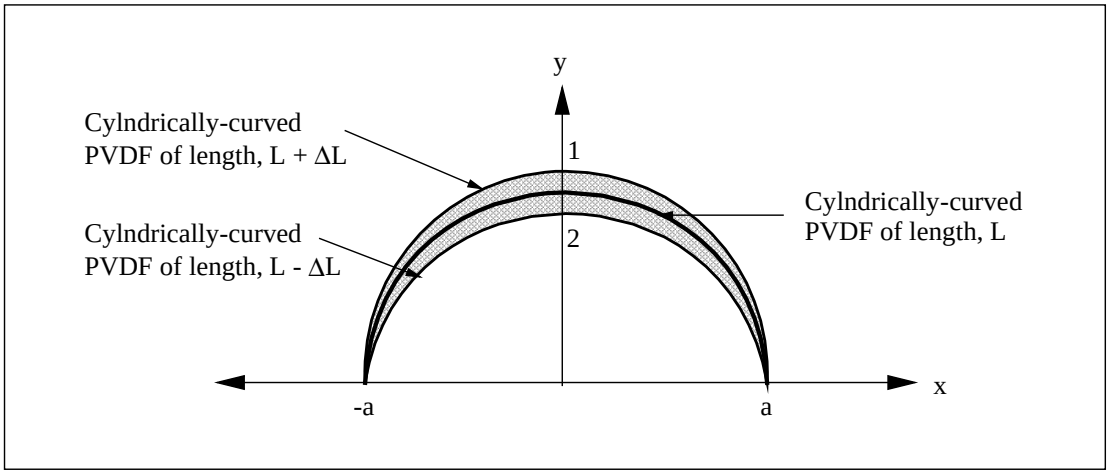

Figure 2.4: Piezo film displacement motion under excitation.

In a preliminary experiment, the smart foam included a continuous, homogeneous layer of PVDF, which was curved into a series of four half-cylinders as shown in Figure 2.5(a). Driving the actuator with an AC voltage across the top and bottom electrode (without changing polarity, as shown in Figure 2.5(a)) resulted in poor radiation efficiency of the active/passive device. When electrically excited, cell 1 and 3 experienced a positive upward displacement. Conversely, cell 2 and 4 experienced a negative downward displacement. The net result is an inefficient sound source at low frequencies with dipole type radiation characteristics. Dipole type radiation characteristics are caused by the relative out-of-phase motion of the neighboring cells. It produces an inefficient radiation pattern because the sound fields generated by neighboring cells partially cancel each other. This inefficient acoustic behavior further manifests itself as higher-order harmonic distortion in the acoustic frequency response spectrum. Specifically, significant sound pressure levels are noted at multiples of the fundamental frequency, the fundamental frequency being the frequency of excitation. Ideally, the sound fields generated by the neighboring PVDF cells should be additive and there should be no harmonic distortion in the acoustic response of the PVDF actuator.

Employing an arrangement first suggested by Tibbets [30], significant enhancements are achieved in the PVDF actuator response. Two improved PVDF actuator configurations are shown in Figure 2.2(b,c). Each actuator is configured by

dividing the continuous layer of PVDF film into several individual transducers by a chemical etching process. The etching process involves chemically removing or erasing thin portions of PVDF film electrodes at the boundaries where the physical polarity (curvature) of the actuator changes. The actuator is then composed of several individual transducers, which can be driven with different voltages (same amplitude with 180° phase difference). In the parallel actuator arrangement, as presented in Figure 2.5(b), the top and bottom electrodes are then connected in parallel with phase reversal. Therefore, the PVDF film is activated such that neighboring cells are driven by the same voltage amplitude with an 180° phase difference. The resulting effect is that each cell moves in the same out-of-plane direction yielding a net volumetric source strength and as a consequence an increase in sound radiation as compared to the preliminary PVDF configuration illustrated in Figure 2.5(a).

The series-parallel actuator configuration, illustrated in Figure 2.5(c), requires that only the bottom electrode is divided into independent transducers, which are then wired 180^{o} out of phase. This arrangement also results in a more efficient radiator as compared to the original configuration as the PVDF film is moving as a whole in the out-of-plane direction. A detailed comparison of the effectiveness of these improved PVDF actuators as sound radiators will be discussed in a subsequent section. Note that the periphery of the PVDF film actuator was etched as well to prevent arcing effects. Electrical leads were attached to the PVDF actuator electrodes with a copper foil adhesive tape reinforced with silver epoxy glue. To complete the construction process of the active-passive control device, the PVDF element was embedded in a layer of polyurethane foam. Note that the piston used in performance testing of smart foam was 15 cm in diameter and dictated the size of the smart foam element to be fabricated. A series of four half-cylinder cells measuring approximately 2 cm in radius were cut through the cross section of a slab of foam measuring 15 cm in diameter and 5 cm thick. Analytical studies concerning curved PVDF acoustic actuators indicate that radius of the PVDF actuator is directly proportional to the acoustic intensity generated by the actuator in the low-frequency range [31]. Therefore, a 2 cm radius is used for each cell as it represents the largest that can be embedded within 5 cm of foam while allowing a minimum of 1/2 cm of foam on the top

and bottom surface of the device for protection of the piezoelectric layer. The PVDF actuator was bonded between the two circular foam halves retaining its curved shape and yielding a smart foam similar to that illustrated in Figure 2.1. Silicon adhesive was chosen to bond the PVDF actuator because it is readily available and remains flexible once dry.

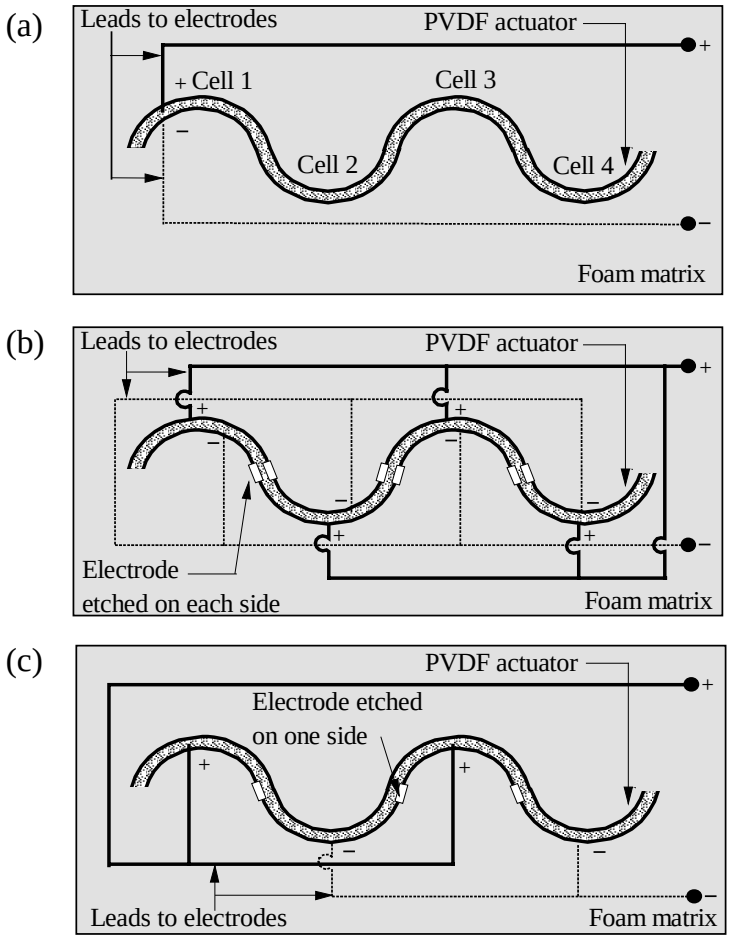

Figure 2.5: PVDF actuator configurations, (a) Original, (b) Parallel and (c) Series-Parallel.

2.4 Piston Radiation Control Experimental Setup & Procedure

The radiation control experimental setup is shown in Figure 2.6. The smart foam was manufactured as described in the previous section and positioned on the surface of an oscillating piston mounted in a rigid baffle inside an anechoic chamber having a cutoff frequency of 250 Hz. The piston excitation is produced by a mechanical shaker driven by an external signal generator. An adaptive feedforward signal processing scheme known as the Filtered-x LMS algorithm [32,33] is used to determine the appropriate control signal necessary to minimize the farfield radiated sound. The error sensor is represented by a ½ in. B&K condenser microphone. This error microphone is located in the farfield at 1.5 m in the perpendicular direction from the smart foam surface (position $\theta=0^o$ in Figure 2.6), and denotes the position of maximum directivity relative to the source. The control algorithm is implemented with a TMS320C30 DSP board resident in a personal computer. Note that the feedforward controller utilizes the signal sent to the piston shaker as a reference signal (however, a signal from an accelerometer on the piston could also be used). A microphone located on a stepper motor driven traverse sweeps from -90^o to 90^o at a radial distance of 1.5 m from the rigid baffle plane for 21 equally spaced measurement points. The farfield sound pressure levels are measured under three conditions:

(1) the bare, untreated piston (*piston*)

(2) the piston with smart foam and no control signal applied (*passive control*)

(3) the piston with smart foam and control signal applied (*active/passive control*)

The recorded sound pressure levels (SPL) in dB relative to 20 μPa are presented for these three conditions to evaluate the efficiency of the passive/active device. A 20 μPa reference is used in all subsequent sound pressure level calculations. The mechanical shaker used to drive the piston appeared to have two resonant frequencies at 290 and 472 Hz in the frequency band studied. Harmonic radiation control implementing smart foam is performed at 290 and 1000 Hz, respectively. These frequencies are chosen to illustrate how the composite smart foam has the ability to successfully attenuate low and high-frequency sound by performing simultaneous passive and active control. In the broadband

control case, the piston is excited with band limited random noise between 100-1600 Hz. Note that for broadband control, a 15 ms delay is added to the disturbance path to make the system causal. It should also be mentioned that, in the following discussion, the term "global" means "for all radiation angles $-90° \le \theta \le 90°$" and "global sound level" refers to the average of the squared sound pressure measured at the 21 equally spaced microphone positions between $\theta=-90^o$ to $\theta=90^o$ and converted to dB relative to 20 μPa.

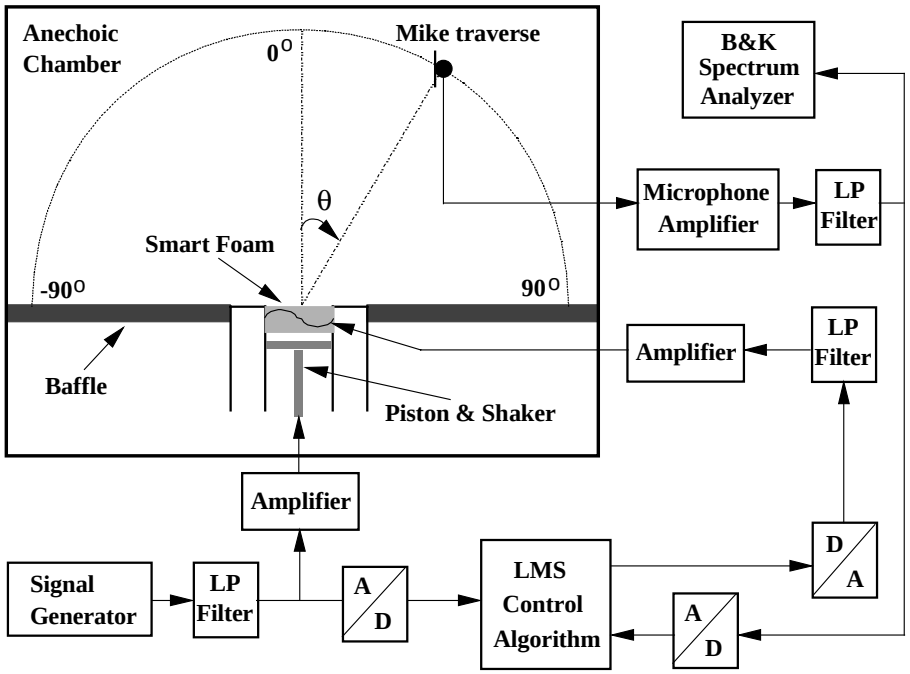

Figure 2.6: Piston radiation control experimental setup.

2.5 Comparison of Acoustic Behavior of Various Actuator Configurations

Linearization of the PVDF actuator acoustic response to an applied voltage proved to be an important achievement in the smart foam development because it is associated with an increased radiation efficiency of the smart foam and therefore an increased sound reduction capability. To illustrate and compare the performance of the different actuator configurations referred to as the original PVDF actuator, the parallel actuator and the series-parallel actuator, a simple experiment is performed in the anechoic chamber. The smart foam is positioned near the surface of the piston and in this case, is used as a noise source (i.e. the piston was stationary and the smart foam was driven with an electrical signal). For the different configurations, the PVDF actuator is driven at 290 Hz using an input voltage of 25, 50, 75 and 100 V_{rms}. Note that the maximum voltage allowed to drive the PVDF actuator is approximately 300 V_{rms}. The farfield sound pressure level (SPL) is measured at the driving frequency as well as at the first and second harmonic frequencies by a microphone positioned normal to the foam surface (at a radial distance of 1.5 m in the direction $\theta=0^{o}$) for each voltage increment.

Figure 2.7(a) presents the SPL for the three different actuator configurations using an input voltage of 100 V_{rms} at 290 Hz. It is observed that the series-parallel and parallel actuators are more than 15 dB louder than the original actuator. The smart foam configured with a parallel actuator yields a higher sound output relative to the series-parallel actuator. This observation is due to the increased electrical power input to the parallel actuator which requires electrical excitation of both the top and bottom surfaces. The linearity of the system with respect to the driving voltage or sensitivity is studied next. The sensitivity, defined as the root mean square (rms) pressure divided by the input voltage is presented in Figure 2.7(b). At the driving frequency, the sensitivity should ideally be a constant (as doubling the driving voltage is expected to double the radiated rms pressure). Indeed, the sensitivity is virtually constant for the three actuator configurations showing that the smart foam is linear with respect to the input voltage. It should also be noted that the sensitivity for the parallel configuration is the highest as it corresponds to the loudest system (see Figure 2.7(a)) and is twice that of the series-parallel configuration. Finally, the non-linear behavior in the form of harmonic distortion

is investigated for the different actuator configurations. Harmonic distortion [34] is a measure of the pressure amplitude distortion and refers to the deviation from correspondence between the acoustic output wave and the electrical input wave that results from nonlinear effects in the smart foam. In this thesis, it is defined as the ratio of the pressure amplitude of the harmonics to those of the fundamental and the harmonics, i.e.,

$$\text{Distortion (in percent)} = 100\sqrt{\frac{p_2^2 + p_3^2 + p_4^2 + \cdots}{p_1^2 + p_2^2 + p_3^2 + \cdots}} \tag{2.1}$$

where p_1 represents the pressure at fundamental frequency, p_2 the pressure at the second harmonic and so on. It can be seen in Figure 2.7(c) that the original actuator configuration is associated with large harmonic distortion (more than 85% when driven with 100 V_{rms}) compared to the other two PVDF actuator configurations. Note that the harmonic distortion associated with the original PVDF actuator configuration was first observed in the piston radiation control experiment presented in [23]. which prompted the search for improved actuator designs. In the current experimental results, it is also observed that the distortion level is increased as the input voltage to the PVDF actuator is increased. Comparatively, the series-parallel actuator corresponds to the best configuration for minimizing the harmonic distortion of the smart foam. In general, the parallel and series-parallel actuator PVDF configurations greatly improve the acoustic response of the smart foam. Both PVDF arrangements yield increased sound output and much less harmonic distortion than the original PVDF configuration.

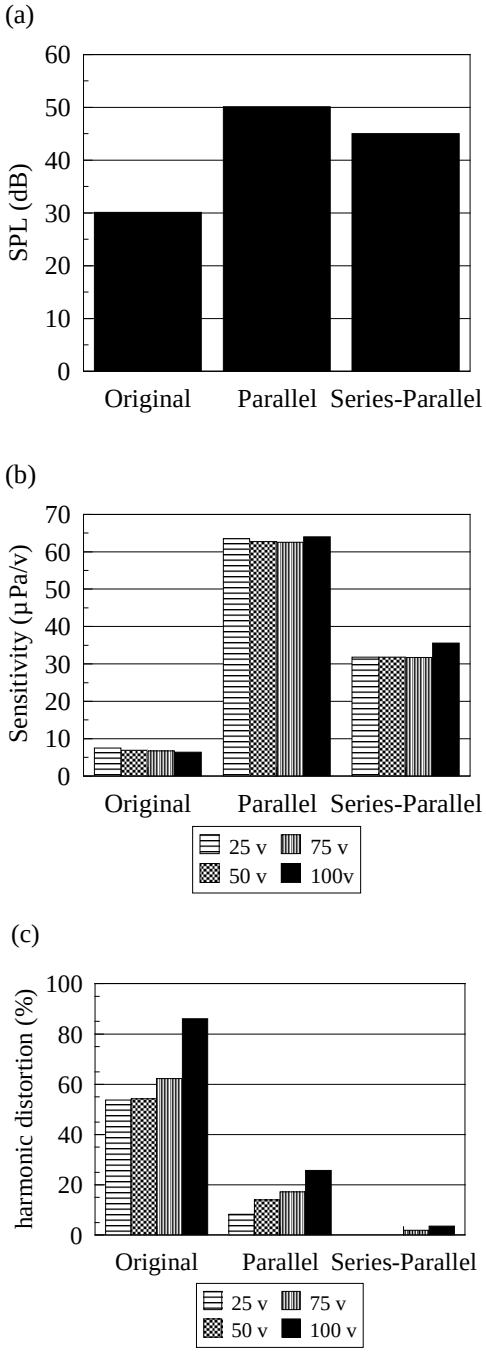

Figure 2.7: Smart foam behavior at 290 Hz for different PVDF actuator configurations (silicone adhesive used); (a) SPL under 100 V rms. input voltage, (b) Sensitivity and (c) Harmonic Distortion

2.6 Passive Effect of Smart Foam on Sound Radiation

In this section, the passive sound attenuation associated with the smart foam is studied and compared to that of a similar configuration of homogenous plain acoustic foam. It is of interest to observe the effect of the PVDF actuator as well as the glue layer (used to bond the PVDF film to the foam) on the passive sound attenuation. Ideally, the passive sound control performance should not be reduced by the active layer embedded in the acoustic foam. A plain, homogeneous layer of acoustic foam (same dimensions as the smart foam) is used for comparison of passive performance. The piston is then driven by broadband random noise (0-1600 Hz) and the global sound level is obtained. Figure 2.8 presents the global sound level for the bare piston (noise source without sound control treatment), for the piston with a plain layer of foam (noise source with common passive sound control treatment) and for the piston with smart foam (no control signal applied to PVDF actuator).

Above 350 Hz, the active layer enhances the passive performance of the acoustic foam. Indeed, in this frequency range, the passive sound attenuation associated with the smart foam is about 15 dB (with respect to the untreated piston source) and that associated with the plain foam is around 6 dB. Obviously, the combined mass of the PVDF and glue layers enhances the passive performance of the acoustic foam as it causes a portion of the energy carried by incident acoustic waves to be reflected back towards the source. In the low-frequency range (below 350 Hz), the plain foam has no effect on the sound radiated by the piston. This is expected due to the longer wavelength of the incident acoustic wave relative to the foam thickness. However, the passive smart foam enhances sound radiation between 200 and 350 Hz. It is suspected that the reason for this phenomena is that the passive smart foam increases the resistive part of the radiation impedance in this frequency range. The radiation resistance is associated with the power radiated away from the source. Placement of the porous smart foam is similar to an attachment of a horn to the piston-like source which results in a marked increase in its acoustic output at low frequencies [35]. In spite of this negative effect in the low-frequency range, the smart foam yields considerable passive sound reduction above 350 Hz..

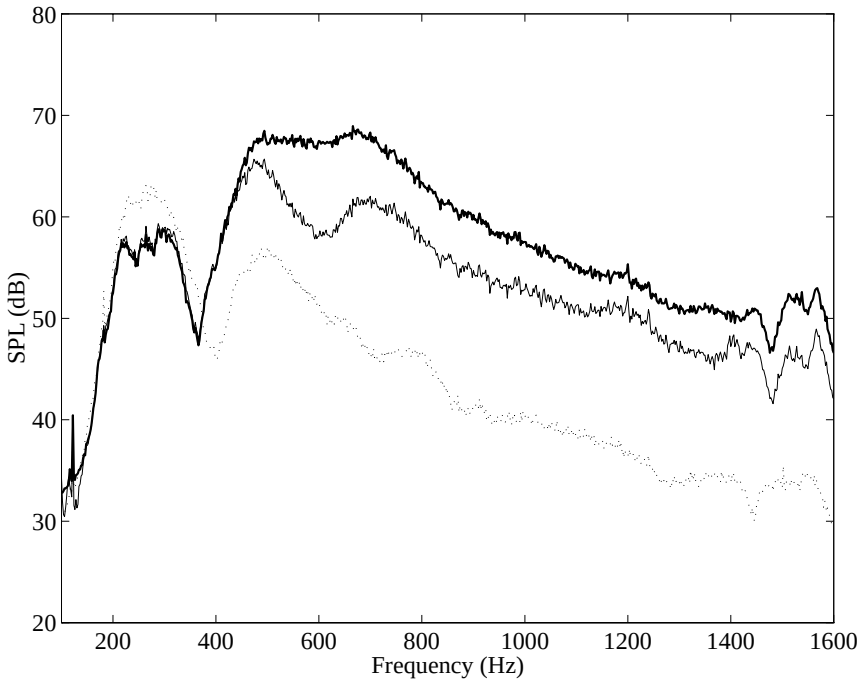

Figure 2.8: Passive effects of embedded PVDF layer on global sound level;
Piston, Plain foam, Smart foam

2.7 Harmonic Radiation Control Results

Harmonic control of piston radiation is investigated for two different excitation frequencies using smart foam. Control results are shown in Figure 2.9 for an excitation frequency of 290 and 1000 Hz, respectively. A 290 Hz excitation frequency corresponds to a resonant frequency of the piston shaker and lies within a frequency range where the smart foam does not provide any passive attenuation. On the other hand, the 1000 Hz driving frequency was chosen because the smart foam provides more than 10 dB of passive sound attenuation at this frequency. In general, the control results show that even if the sound radiation is minimized at only one location in space (direction θ=0°), the sound attenuation under control is global. In Figure 2.9(a), the global sound level is decreased by about 20 dB at 290 Hz using the series-parallel actuator. The parallel actuator yields a 16 dB global sound reduction. It is also observed that at this frequency, the passive smart foam causes a 1.5 dB increase in the farfield radiation. The reason for this behavior is an increase in the radiation resistance under passive control as pointed out in the previous section. Figure 2.9(b) shows results for a 1000 Hz excitation frequency.

About 10 dB passive sound reduction is observed while a further 10 dB global reduction is attributed to the active PVDF actuator. The global noise cancellation was obtained as the smart foam is able to change the radiation impedance seen by the vibrating piston. The attenuation achieved by both PVDF actuator configurations is comparable at this frequency. Radiation control at other harmonic excitation frequencies were investigated and indicated that the series-parallel actuator performed best at reducing the piston sound radiation. However, it is important to note that the control voltage required by the series-parallel configuration is greater than that needed by the parallel actuator. For example, for a 290 Hz drive frequency, the series-parallel actuator required about 1.5 time more voltage than the parallel actuator to minimize the piston radiation. This observation was expected as Figure 2.7(a) illustrated that the parallel actuator was a more efficient sound radiator than the series-parallel actuator. At 1000 Hz, where passive sound absorption is evident, the control voltage required to drive the PVDF actuator was much lower than at 290 Hz. Therefore, as the piston excitation frequency increases, the passive absorption provided by the smart foam increases and the voltage required to drive the PVDF actuator decreases. Applying the maximum allowable control voltage (i.e. 300 V_{rms}) would allow the smart foam to radiate a 60 dB sound pressure level at 1.5 m at 290 Hz using the parallel configuration. For the same type of excitation, a 71 dB sound pressure level can be generated by the smart foam at 1000 Hz. It is useful to relate the radiated pressure to the velocity of the smart foam surface by quantifying the source strength, i.e. the product of the velocity multiplied by the surface area of the source [36]. Two assumptions are made to estimate the source strength of the smart foam at the frequencies studied. First, it is assumed that the relationship between the pressure, $p(r)$, and the particle velocity, $u(r)$, is defined by the expression $u(r) = p(r)/\rho_o c_o$. (Note that $\rho_o c_o$ is the characteristic impedance of air). Second, it is assumed that the velocity of the air at the smart foam-air interface exactly matches the velocity of the smart foam surface. Accordingly, the equivalent source strength at 290 Hz and 1000 Hz are 3.5×10^{-6} m^3/s and 12.5×10^{-6} m^3/s, respectively.

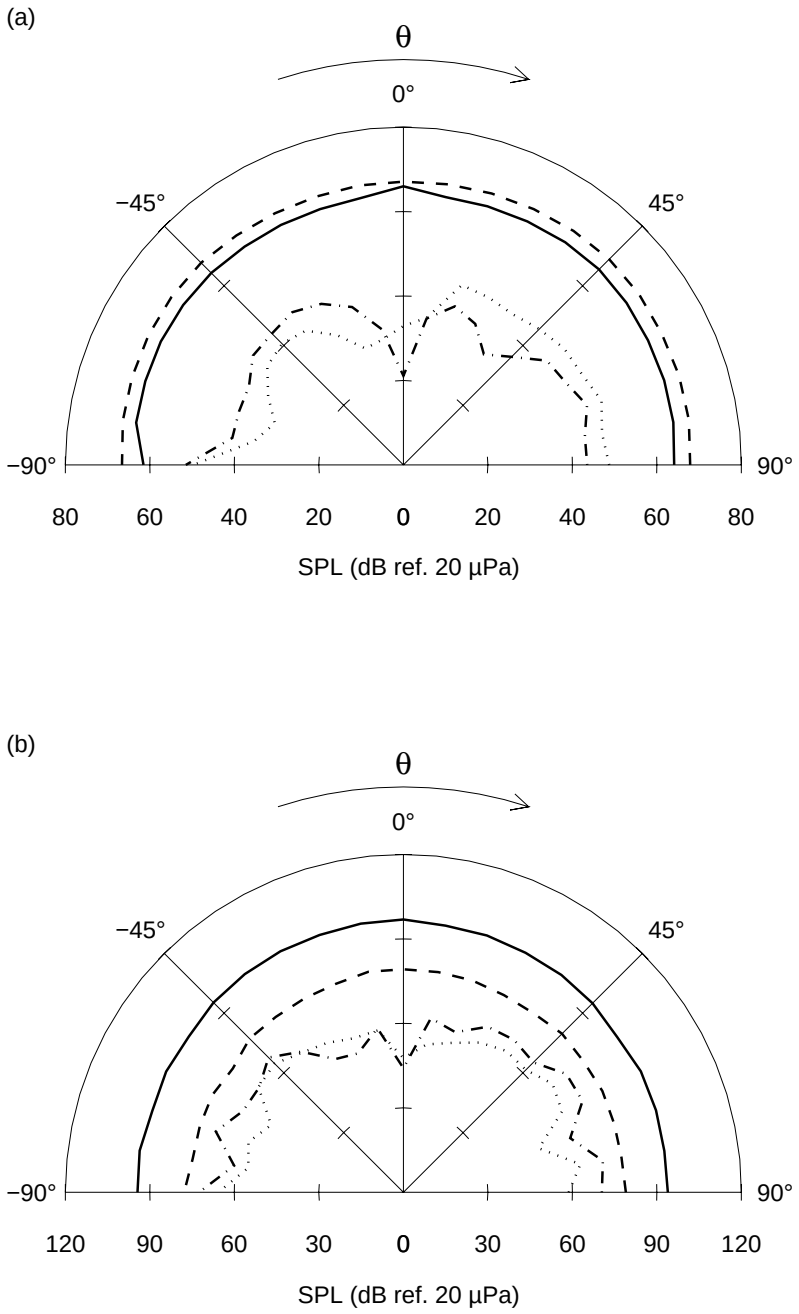

Figure 2.9: Harmonic control results at (a) 290 Hz and (b) 1000 Hz; —— Piston, – – – Passive, – · – · Active/Passive series-parallel configuration, ····· Active/Passive parallel configuration.

In the interest of developing a compact smart foam actuator and error sensor configuration, an attempt was made to implement a PVDF error sensor mounted on the surface of the foam. In this experimental study, a sheet of PVDF was bonded to the

surface of the smart foam and emitted a voltage output proportional to the mechanical strain integrated over the surface. Note that the acoustic component of smart foam was not measured by the distributed sensor. The goal was to achieve farfield sound reduction of harmonic piston radiation by minimizing the PVDF error signal. Success of this approach would eliminate the need of a farfield error microphone. Unfortunately, this setup did not yield any sound attenuation indicating that the integrated surface strain of the dual-phase foam is not directly related to the volume velocity of the foam surface. This correlation is necessary to achieve satisfactory attenuation of farfield sound radiation. It is suspected that the reason for the poor performance is that the motion of the PVDF actuator within the foam during control is not perfectly piston-like. This may contribute a slight shearing effect within the foam which would distort the error signal. Furthermore, the foam surface has a structural and acoustic phase which contribute to the volume velocity of the system, however, the PVDF error sensor only measures mechanical strain. This means that the acoustic component contributing to the radiated power of the system is not accounted for in the error information measured by the PVDF sensor.

2.8 Broadband Radiation Control Results

In this section, the performance of smart foam as a broadband control actuator is investigated in terms of piston sound radiation control. In the experiment, the piston is excited with band-limited random noise having a frequency content of 100-1600 Hz. As in the harmonic control case, the error microphone is located in the direction perpendicular to the surface of the foam (1.5 m away in direction $\theta=0^o$). This error microphone position represents the location of maximum directivity. The performance of the smart foam for minimizing broadband piston radiation at the error microphone is illustrated in Figure 2.10(a). In terms of passive control performance of the smart foam actuator, below 400 Hz, the passive smart foam initiates a slight increase in sound radiation compared to the untreated piston sound levels. This low-frequency increase in sound output indicates that the passive acoustic foam produces a “horn-like” effect in front of the piston by reducing the area of air flow. Below 400 Hz, an active sound

attenuation of about 10 dB is achieved using the parallel actuator configuration and approximately 15 dB gained with the series-parallel configuration compared to the passively treated piston. In this low-frequency range, it is important to note that the active component (PVDF actuator) is able to compensate for the inability of the smart foam to provide passive sound attenuation. Between 400 Hz and 1600 Hz, the high-frequency dissipative mechanisms offered by the passive foam is evident as it yields approximately 15 dB passive sound reduction across the frequency bandwidth. Similarly, in this higher frequency bandwidth, the series-parallel actuator configuration performs better than the parallel configuration. This is believed to be related to the non-linear behavior associated with the parallel configuration (as seen in Figure 2.7(c)). In this high-frequency range, compared to the passive control case, a further 10-15 dB attenuation is associated with the active contribution of the series-parallel PVDF element. With regard to the smart foam configured with a parallel PVDF configuration, a further 3-5 dB attenuation is observed between 400 Hz and 1600 Hz. It was again noticed that the control signal used to drive the PVDF actuator (for all configurations) decreases in amplitude as the frequency increases owing to the increased sound attenuation offered by the passive acoustic foam. .

Global sound levels associated with the active/passive smart foam are presented in Figure 2.10(b). The global passive control performance is similar to that observed at the error sensor. No passive reduction is noted below 400 Hz, however, approximately 15 dB passive sound reduction is achieved above this frequency. Below 900 Hz, the smart foam with an embedded parallel PVDF configuration offers a further 5 dB active sound reduction compared to the passive control results. In the same frequency range, the smart foam with an embedded series-parallel PVDF configuration offers a further 10 dB active sound reduction compared to the passive control results. Above 900 Hz, the amount of active reduction offered by both PVDF configurations seems to decrease and slight control spillover occurs. This may be attributed to the very low sound levels of the passively controlled piston and the beginning of less “monopole-like” behavior of the control actuator in the high-frequency range.

(a)

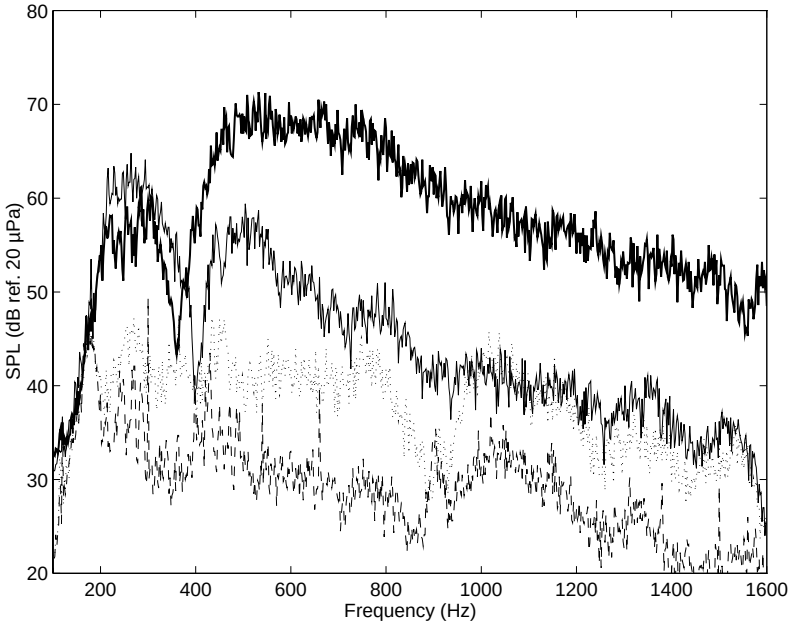

(b)

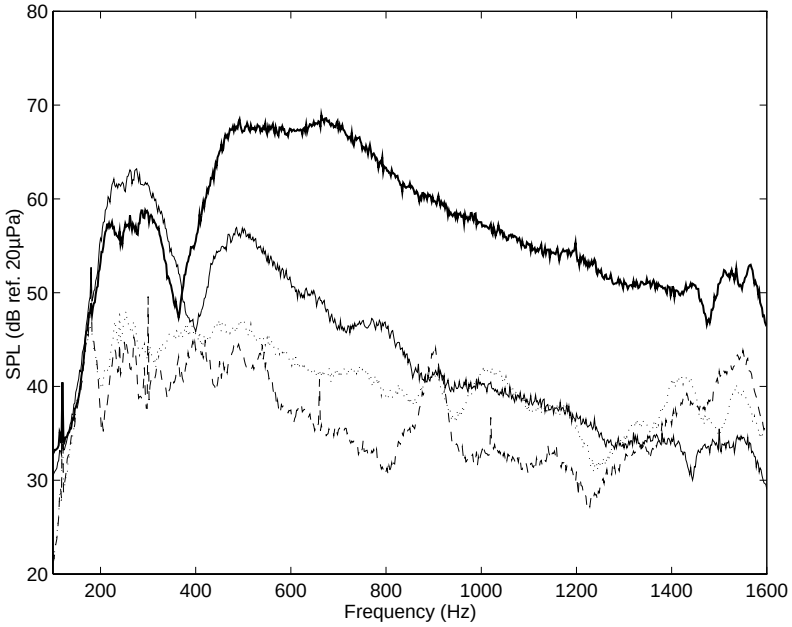

Figure 2.10: Broadband control results; (a) SPL at error microphone;
(b) global sound level; ━━━ Piston, ——— Passive, - - - - - - - - - Active/Passive series-parallel configuration, ····· Active/Passive parallel configuration.

The previous broadband control results indicate that global active/passive sound attenuation of the piston radiation is achieved by employing one smart foam actuator and a single error microphone. Even though some control spillover is present in the high-frequency range, the sound levels never increase above that of the untreated piston. Thus, the passive sound dissipation associated with smart foam provides some fail-safe control.

2.9 Feasibility of Implementing a Nearfield Error Microphone

In many active noise control applications, the use of farfield error sensors is not practical. With this in mind, an experiment is performed to determine how close to the smart foam surface an error microphone could be placed and still be able to yield significant farfield sound reduction. In the experiment, the piston was excited with band-limited random noise (frequency content 0-1600 Hz). A smart foam actuator having a series-parallel configuration is used. A microphone is located in the farfield at 1.5 m and $\theta = 0^o$, directly in front of the piston/smart foam system. This microphone is used to "monitor" the sound pressure level while a nearfield microphone is used to provide an error signal for the control algorithm. Independent experiments are conducted where the error microphone is located at several positions between 3.0 cm and 15.0 cm from the smart foam surface. An error microphone located at 15 cm yielded the highest amount of farfield attenuation in the frequency range studied. This was expected since a 15 cm distance is comparable to the diameter of the system and allows the sound radiating through the entire smart foam surface to be measured by the nearfield error sensor. Figure 2.11 compares the global active-passive sound reduction achieved by implementing nearfield or farfield control. It is generally observed that each error sensor configuration yields considerable global sound reduction between 150 and 1200 Hz. Above 1200 Hz, some control performance degradation is noted but this can be dealt with by terminating the active control input and allowing the passive reduction offered by the foam to provide high-frequency sound reduction. These results are promising and show the potential for having an integral smart foam actuator/error sensor radiation control system.

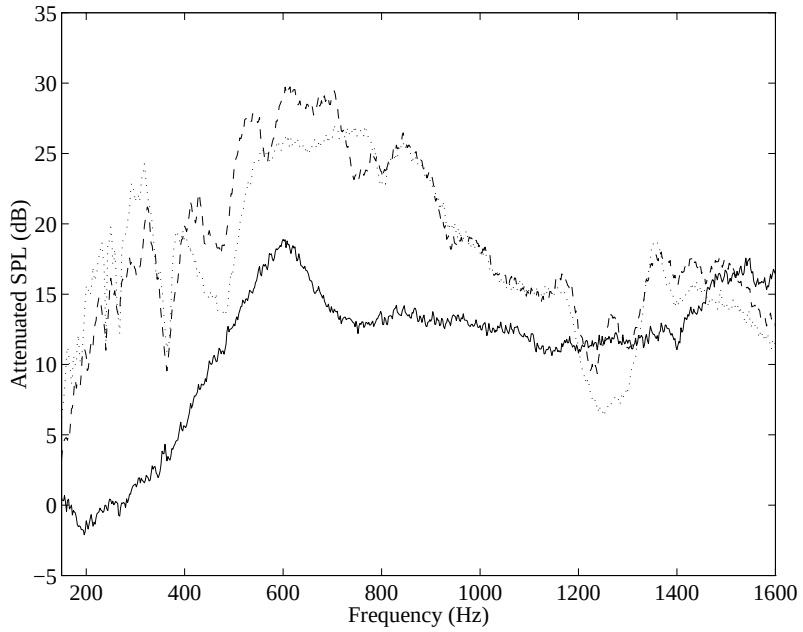

Figure 2.11: Comparison of global sound attenuation offered by nearfield and farfield error sensors;
——— Passive, -------- Active/Passive (farfield control), ... Active/Passive (nearfield control).

2.10 A Note about Smart Foam Bonding Layer and Lead Attachment

Two further improvements of smart foam subsequent to the experimental study described in this chapter were discovered. Riveted crimp connectors made of copper proved to be an improved lead attachment method because it has a small contact area and seems to be more reliable at high voltages than copper foil tape. Furthermore, the acoustic behavior of a smart foam constructed with spray glue adhesive was investigated. It was suspected that the harmonic distortion can be further decreased by using a much thinner bonding layer between the PVDF actuator and the foam. Silicone adhesive has a high viscosity compared to spray glue adhesive. This high viscosity can induce a shearing effect in the smart foam, which promotes a nonlinear coupling of the PVDF in-plane strain and the displacement in the normal direction. The sound radiation and sensitivity exhibited by the three types of smart foam actuators, measured using the same experimental setup outlined in section 2.5, are shown in Figure 2.12. An actuator constructed with spray glue yielded negligible nonlinear distortion. A comparison of

sound pressure levels and sensitivities of an actuator manufactured with spray glue or silicon adhesive are presented in Figure 2.7 and Figure 2.12. These plots reveal that a smart foam assembled with spray glue adhesive, which provides a very thin bonding layer, has a higher radiation efficiency for the same input voltage.

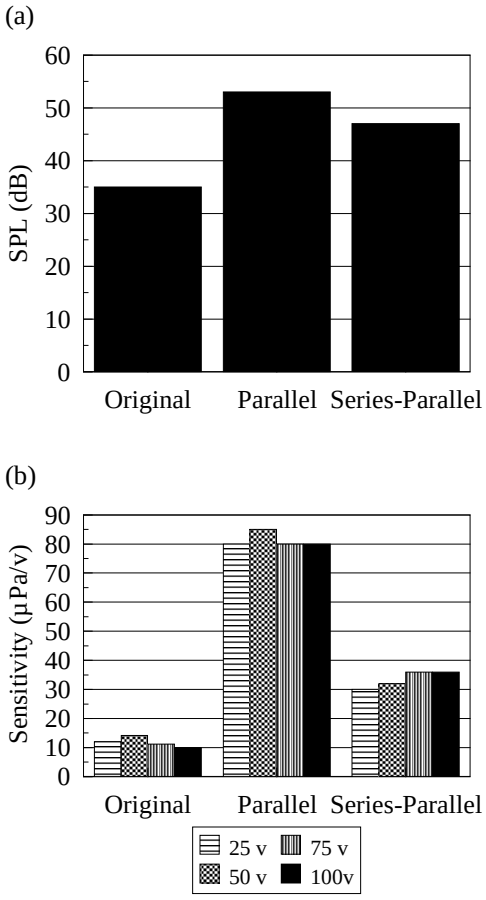

Figure 2.12: Smart foam behavior at 290 Hz for different PVDF actuator configurations (spray glue adhesive used); (a) SPL under 100 V rms. input voltage, (b) Sensitivity and (c) Harmonic Distortion.

Another important advantage of using a thinner bonding layer relates to the weight of the actuator. One of the goals in smart foam development is to keep the weight of the actuator to a minimum. The surface density of a homogeneous layer of foam used in this study is 1.6 kg/m^2. The surface density of smart foam assembled with silicone adhesive is 4.5 kg/m^2, and the surface density of smart foam made with spray glue is 2.0 kg/m^2. The weight of the actuator is reduced by more than 50% when a thin bonding layer is used. Consequently, in future experiments, all smart foam actuators are constructed using riveted crimp connectors and a spray glue adhesive.

2.11 Summary

A sound absorbent foam with an embedded piezoelectric PVDF layer known as smart foam has been introduced as a active/passive noise control device, which has many advantages over conventional noise attenuation systems. Numerous smart foam design improvements are discussed and implemented to decrease the smart foam nonlinear response and increase its' sound radiation. Global cancellation of harmonic and broadband noise induced by a simple source was successfully achieved by the smart foam. The potential of smart foam to globally reduce low-frequency and high-frequency sound while minimizing the nearfield or farfield sound pressure was also illustrated.